Catchment-scale herbicides transport: theory and application

E. Bertuzzo[a,*], M. Thomet[a,b], G. Botter[c], A. Rinaldo[a,c]

[a] *Laboratory of Ecohydrology, School of Architecture, Civil and Environmental Engineering, Ecole Polytechinque Fédérale de Lausanne (EPFL), 1015 Lausanne, Switzerland*

[b] *e-dric.ch, 1015 Lausanne, Switzerland*

[c] *Dipartimento di Ingegneria Civile, Edile ed Ambientale, Universitá di Padova, 35131 Padua, Italy*

Abstract

This paper proposes and tests a model which couples the description of hydrologic flow and transport of herbicides at catchment scales. The model accounts for streamflow components' age to characterize short and long term fluctuations of herbicide flux concentrations in stream waters, whose peaks exceeding a toxic threshold are key to exposure risk of aquatic ecosystems. The model is based on a travel time formulation of transport embedding a source zone that describes near surface herbicide dynamics. To this aim we generalize a recently proposed scheme for the analytical derivation of travel time distributions to the case of solutes that can be partially taken up by transpiration and undergo chemical degradation. The framework developed is evaluated by comparing modelled hydrographs and atrazine chemographs with those measured in the Aabach agricultural catchment (Switzerland). The model proves reliable in defining complex transport features shaped by the interplay of long term processes, related to the persistence of solute components in soils, and short term dynamics related to storm inter-arrivals. The effects of stochasticity in rainfall patterns and application dates on concentrations and loads in runoff are assessed via Monte Carlo simulations, highlighting the crucial role played by the first rainfall event occurring after herbicide application and yielding a probabilistic framework for critical

*Corresponding author

Email address: enrico.bertuzzo@epfl.ch (E. Bertuzzo)

determinants of exposure risk to aquatic communities. Modeling and monitoring of herbicides circulation at catchment scale thus emerge as essential tools for ecological risk assessment.

Keywords:
herbicide transport, travel time, residence time, atrazine

---

1. Introduction

Catchment hydrologic response to rainfall forcings – here including fluxes of both water and solutes – involves both event (new) and non-event water stored in the catchment, possibly for rather long times, mixed in different proportions depending on the hydrologic pathways involved in runoff formation. Indeed, the mixing of water of different ages has been argued to dominate the variability of water quality in the runoff [1–3]. This stems from the fact that the chemical composition of streamflows is driven by the water residence time in the catchment which quantifies the time available for chemical, biological and physical processes to modify the original composition of inputs through gain or loss [e.g. 4–8]. However, some of the processes controlling the release of pre-event water from catchments are still poorly understood and rather roughly modeled, and the observational data do not suggest either simple, much less universal, behaviors [9–12]. The complexity of the mixing patterns involving event and pre-event waters in catchments is partly a byproduct of the structural complexity of intertwined surface and subsurface hydrologic environments, which are typically characterized by pronounced heterogeneity. Within such contexts, the probabilistic characterization of travel times to a control surface (possibly conditional on injection times [13]) provides a robust and integrated stochastic description of how catchments retain and release water [9, 10, 12, 14–20].

Unerringly solute flux concentrations (i.e. the ratio of instantaneous mass flux and flow discharge) measured in catchment runoff depends on the mixing of water from different sources, ages and chemical compositions. Highly fluctuating concentrations in surface waters are observed, resulting in complex, histeretical relations with discharge. In the case of pollutants like herbicides, whose lifetimes and mobility in surface and subsurface waters has long been studied [e.g. 8, 21–31], fluctuating concentrations and their peaks (and duration) over a toxic threshold are crucial to assess the ecological risks to aquatic communities [32–34].

The assessment of catchment-scale mobility of herbicides is deemed a relevant endeavor because the use of crop protection agents is commonplace in modern agriculture. Therefore the problem of herbicides transported from the soils where they are applied to surface and groundwater is emerging as a critical factor for a variety of environmental hazards. In the last years great interest was placed in developing measures to minimize herbicide losses from agricultural fields to surface waters [e.g. 31]. Measures to reduce the damage due to herbicide losses range from the alternative use of products less harmful to the environment, to alternative field management strategies. Studies have focused on the parts of the catchment contributing more decisively to surface water pollution [35–37]. In particular, it has been shown that more than 80% of the total herbicide losses from small Swiss-catchments occurred during the first two rain events following application [38]. This is a recurrent pattern, owing to the intrinsic decay rates of pesticides and herbicides. Moreover, the influence of the variability of field-specific characteristics on total herbicide loads proves much larger than the difference in compound-specific properties, as indeed hydrologic factors tend to dominate the spatial distribution of losses [36, 37].

While important for management purposes, the above approaches do not address the issue of fluctuating concentrations in the streamflow. Indeed a full understanding of the transport of reactive chemicals such as herbicides adds layers of complexity to the features of the hydrologic response. This is contributed, in particular, by soil biogeochemistry that affects herbicide sorption and degradation, and by land use/cover and soil/crop management practices, i.e. crop distribution and growth, planting dates, timings and rates of pesticide applications [8]. Limited effective mobility at catchment scales may emerge [36] as it has been observed that on average only about 1% of applied atrazine mass is exported on an annual basis from catchments covering nine orders of magnitude [39]. This, among other consequences, implies that in-stream processing of, say, atrazine is negligibly small, and that much of the atrazine applied is either retained or transformed in the soils. Herbicides reach surface waters through runoff and drainage mostly during and immediately after rain events, resulting in highly time-variant river concentrations. Hence, the input of herbicides into aquatic environments often occurs in pulses rather than via smooth continuous flows, producing highly erratic exposures of aquatic life to dangerous concentrations. Traditional ecological risk assessments do not reflect this fundamental time-varying character of exposure to herbicide concentrations, mostly because toxicity experiments are

based on continuous exposure of an organism to a single pollutant [40]. The fluctuating character of pollutant exposure prompts new approaches to the ecological risk [32–34], for which extended monitoring is not a cost-effective option because of the high frequency needed to describe the temporal dynamics of herbicide concentrations, and the related often unmanageable costs of herbicide analysis.

Modeling and monitoring are thus seen as essentially complementary tools for any assessments of water quality. In particular, we direct our efforts towards predicting instantaneous herbicide concentrations in the hydrologic response at the closure of a catchment. This paper addresses the coupling between hydrologic and transport models through the quantification of water flow and solute transport in the general framework of the formulation of transport by travel time distributions [5, 6, 13]. To this aim we generalize a recently proposed scheme for the derivation of travel time distributions [13] to the case of solutes like herbicides, which are not completely taken up by transpiration and undergo chemical degradation. Section 2 provides the analytical derivation for a single hydrologic control volume forced by generic input and output fluxes. This general solution can be readily particularized and applied to more complex and specific hydrologic schemes comprising different control volumes in series or in parallel. This is the case of the application presented in Section 3 where a complete model for flow and atrazine transport in the Aabach basin (Switzerland) is developed and tested in a comparative mode with the extensive experimentation carried out therein [27, 35, 36, 38, 41]. The effects of stochasticity in rainfall patterns and application dates on concentrations and loads in runoff are assessed via Monte Carlo framework. The results of this analysis are discussed in the perspective of a new approach to ecological risk assessment (Section 4). A set of relevant conclusions close the paper (Section 5).

2. Theoretical Framework

2.1. Travel Time Formulation of Transport

Let us start by considering a control volume V (see Fig. .1), which can at first be thought of as a hillslope but it can be readily generalized to any suitable sub-unit of a more complex hydrologic scheme. The macroscopic balance of water storage $S(t)$ depends on input $I(t)$, outflow $Q(t)$ and evapotranspiration $ET(t)$. As an example, if the control volume is aimed to describe the

dynamics of a superficial layer, the term $I(t)$ represents inputs form precipitation. In the case a deeper layer is considered, inputs are mainly constituted by infiltration from the upper layers. We differentiate the total output between outflow $Q(t)$ and evapotraspiration $ET(t)$ because we consider in the follow the case where selective transpiration can change solute concentration in the storage. Analogously, the mass of solute $M(t)$ stored in the control volume depends on the solute fluxes $\phi_I(t)$, $\phi_Q(t)$ and $\phi_{ET}(t)$ associated to $I(t)$, $Q(t)$ and $ET(t)$, respectively. The volume and mass balance thus read

$$\frac{dS(t)}{dt} = I(t) - Q(t) - ET(t)\,, \tag{1}$$

$$\frac{dM(t)}{dt} = \phi_I(t) - \phi_Q(t) - \phi_{ET} + \mathcal{R}\,, \tag{2}$$

where $\mathcal{R}$ defines a generic exchange term affecting the mass balance of reactive solutes involved in biological, chemical or physical transformations (e.g. biogeochemical cycling, chemical degradation or any mass transfer from mobile or immobile water or soil phases).

The framework derived herein fully exploits recent advances in the description of transport process via travel and residence time distributions [13, 42, 43]. We define as $p(t|t_i)$ the probability density function of the timespan elapsed between the entrance of a water particle within V as I and its exit through any boundary of the control volume as Q or ET. Hence $p(t|t_i)\,dt$ represents the fraction of water particles entered at time t_i that exits in the time interval $[t_i + t, t_i + t + dt]$. The notation empathizes that this timespan depends on the temporal evolution of input forcing, storage and evapotranspiration, and thus on the particular injection time t_i at which the particles may enter the system. Accordingly let $P(t|t_i)$ be the conditional exceedance cumulative probability (i.e. $P(t|t_i) = 1 - \int_0^t p(x|t_i)dx$). By definition the quantity $P(t - t_i|t_i)$ represents the probability that a water particle entered at time t_i is still within the control volume at time $t \geq t_i$. Thus the instantaneous water storage $S(t)$ can be expressed as:

$$S(t) = \int_{-\infty}^{t} I(t_i)P(t - t_i|t_i)dt_i\,. \tag{3}$$

To differentiate between the two possible fates of a water particle, we define the travel time T_t and the evapotranspiration time T_{et} as the time elapsed between the injection and the exit as Q and ET, respectively. Analogously

to the case of $p(t|t_i)$, T_t and T_{et} are described by their conditional probability density functions (pdf), $p_t(t|t_i)$ and $p_{et}(t|t_i)$. We term $\theta(t_i)$ the probability that a water particle injected in the time interval $[t_i, t_i + dt_i]$ will exit the control volume V as Q, while with the remaining probability $1 - \theta(t_i)$, the water particle will leave as evapotranspiration. Therefore, the probability density function $p(t|t_i)$ can be expressed as a linear combination of travel and evapotranspiration time pdfs: $p(t|t_i) = \theta(t_i)p_t(t|t_i) + [1 - \theta(t_i)]p_{et}(t|t_i)$. Comparing the time derivative of Eq. (3) with Eq. (1) and partitioning the flow between discharge and evapotranspiration, one finally gets relations:

$$Q(t) = \int_{-\infty}^{t} I(t_i)\,\theta(t_i)\,p_t(t - t_i|t_i)\,dt_i\,, \tag{4}$$

$$ET(t) = \int_{-\infty}^{t} I(t_i)\,[1 - \theta(t_i)]\,p_{et}(t - t_i|t_i)\,dt_i\,. \tag{5}$$

Eq. (4) could erroneously recall the classical convolution between effective rainfall and instantaneous unit hydrograph; however, they are mathematically and physically profoundly different. Mathematically, the difference is related to the time variant nature of the travel time pdf that changes depending on the injection time t_i. From a physical viewpoint, while the unit hydrograph quantifies the effect of a given event in terms of discharge, and is thus related to the speed at which the hydrologic signal propagates within an hydrologic unit, the travel time distribution reflects the age of the water and is controlled by pore water velocity and by mixing processes involving old and event water [11, 13].

The above scheme may be readily generalized to describe transport processes of reactive and passive solutes in the hydrologic cycle. To this aim, it is further assumed that the solute concentration of a given water input inside V depends on the time spent inside the control volume regardless of the particular trajectories followed by water particles and regardless of their position within V. Under the above assumption, the solute concentration C of a water input at a given time t depends only on the injection time t_i and on the time $t - t_i$ spent inside V by the particles (i.e. $C = C(t - t_i, t_i)$, $t \geq t_i$). Analogously to the derivation of Eqs. (3) and (4), the mass storage $M(t)$ and the mass flux associated to the outflow $\phi_Q(t)$, can be expressed as

$$M(t) = \int_{-\infty}^{t} I(t_i)C(t - t_i, t_i)\,P(t - t_i|t_i)\,dt_i \tag{6}$$

$$\phi_Q(t) \;=\; \int_{-\infty}^{t} I(t_i)C(t-t_i,t_i)\theta(t_i)\,p_t(t-t_i|t_i)\,dt_i\,. \tag{7}$$

This general framework will be particularized in the following to derive the specific transport model used.

2.2. Mixing Assumption

In order to derive the travel time distribution, specific assumptions on the mixing of water particles inside the control volume are needed. Botter et al. [13] derived the pdf $p_t(t|t_i)$ and $p_{et}(t|t_i)$ under a well-mixed assumption, i.e. particles that exit as ET or Q are randomly sampled among all the water particles inside V. Despite its simplicity, this assumption proved able to satisfactorily capture broad features of transport processes even in heterogeneous settings. In particular Rinaldo et al. [43] carried out a detailed comparison of travel times within a hillslope-channel system computed via complete numerical model with those evaluated by the approach described here. It was argued that the robustness of the well-mixed assumption – in the particular case therein and owing to general theoretical issues – is supported by the integrated nature of the kinematic quantities employed in the travel time formulation of transport and by its non-point source nature. Moreover, it must be noticed that one can combine (in series and/or in parallel) different well-mixed control volumes into more realistic hydrologic scheme. The only requirement is that once a particle leaves V it cannot reenter the system at later times (absorbing boundaries).

Under the well-mixed assumption, The travel time pdf $p_t(t-t_i|t_i)$, $t > t_i$ can be expressed as (see Appendix A for the full derivation)

$$p_t(t-t_i|t_i) = \frac{Q(t)}{S(t)\theta(t_i)} e^{-\int_{t_i}^{t} \frac{Q(x)+ET(x)}{S(x)} dx}\,, \tag{8}$$

where $\theta(t_i)$ is the normalization factor (Appendix A). Notice that the solution (8) depends only on the time evolution of water storage, outflow and evapotranspiration after the injection time t_i.

2.3. Solute Transport

In the present study we account for the different affinity shown by different types of solutes to leave the system through transpiration. A general approach is considered by defining the concentration of the evapotranspired water $C_{ET}(t-t_i,t_i) = \alpha(t)\,C(t-t_i,t_i)$ with $\alpha(t) \in [0,1]$. This allows one to

consider intermediate cases where $C_{ET}(t-t_i, t_i)$ is lower than the corresponding soil solute concentration ($C(t-t_i, t_i)$). Solutes can be taken up by plants in the transpiration water and therefore the value of the parameter α chiefly depends on the ratio between transpiration and evaporation and on the type and stage development of the transpiring plants. These last two factors can change seasonally and we thus derive the solution in the general case where α is time dependent. The two extreme cases are $\alpha \equiv 0$ where no solute is transpired and $\alpha \equiv 1$ where the ET flux has the same concentration as the soil water. When $\alpha < 1$ the solute concentration in the soil changes due to solute enrichment by evapotranspiration. In addition to this physical process we account also for a linear decay/degradation at a rate k which describes fairly well the behaviour in the soil of many solutes of practical interest.

Accounting for selective transpiration, solute degradation and the non stationary travel time distributions induced by a well-mixed dynamics, the mass flux of solute associated to the flow Q reads (see appendix B for the full derivation):

$$\phi_Q(t) = \int_{-\infty}^{t} I(t_i) C_I(t_i) \frac{Q(t)}{S(t)} e^{-\int_{t_i}^{t} \frac{Q(x)+\alpha(x)\,ET(x)}{S(x)} dx - k(t-t_i)} dt_i \,, \tag{9}$$

The generality of the solutions (8) and (9) stems from their applicability regardless of the particular hydrologic model or measurement used to estimate the relevant fluxes. In the following we develop a specific hydrologic model to apply this framework to the herbicides case study.

3. Application: Herbicide Concentrations in the Aabach Catchment

3.1. Data

The framework developed in section 2 is applied to model herbicide transport in a Swiss agricultural catchment. An important field measurement campaign including high frequency measurement of discharges and of the flux concentrations for several herbicides was carried out in 1999 for the basin of the Greifensee [40, 44]. The case study presented focuses on catchment-scale circulation of atrazine because this herbicide is only used for corn protection and thus has a single and more identifiable source [26, 35]. The study catchment, Aabach-Mönchaltorf, is part of the catchment of Lake Greifensee east of Zürich. Concentration and discharge are measured in the Aabach creek

at the closure located in the village of Mönchaltorf. The catchment has an area of $A = 46$ km^2 and is covered mainly by agricultural land (Fig. .2a). A sample of the temporal dynamics of discharge and atrazine concentrations in the Aabach stream at Mönchaltorf is shown in Fig. .2b. Atrazine samples were taken proportionally to water volumes. During rain events the sample frequency is 20 minutes, in case of low discharges the frequency is reduced to two hours. The sampling period is then divided into equal flow volume timespans, whose duration ranges from 1 to 24 days. Samples belonging to the same timespan are then mixed and the mean concentration is measured. At seasonal timescale, the temporal evolution of atrazine concentrations shows a sudden increase after the application that occurred in the May-June period, followed by a slow decay due to the persistence of atrazine in the system. Zooming at sub-seasonal timescale, it is interesting to note that the concentration peaks are rather synchronous to discharge peaks, suggesting the mobilization of atrazine by rainfall events.

The total atrazine mass applied during the survey is 140 ± 1 kg [44], but the application dates are not exactly known. Atrazine application has been assumed to be restricted to the period before June the 30^{th}, as prescribed by Swiss law. After considerations regarding weather conditions, trafficability of the fields and behavior of the atrazine concentration measurements, the application dates can safely be restricted to two short time windows around April 25 and May 15. Upon interviews with farmers, the relative fraction of mass applied has been approximately set to 1/4 and 3/4 of the total for the first and the second application dates, respectively.

Freitas et al. [36] experimentally determined the apparent distribution ratio (K_d) and half-lives (DT_{50}) for four fields in the Ror-catchment, a subcatchment of the Aabach basin investigated in the present study. K_d is the ratio of concentration of the herbicide sorbed to soils (N) and the dissolved concentration (C). The values found are in the range of $K_d = 2.2 - 17$ $[l/kg]$ up to 32 days after application. The half-lives of the herbicides in the soils were also estimated based on the decay of the total mass (sorbed and dissolved) until 32 days after application. The data was fitted to a first order degradation function $C(t) = C_0\, exp(-k\, t)$, where $k[d^{-1}]$ is the dissipation constant corresponding to $\ln(2)/DT_{50}$. Half-lives experimentally found by range between 12 and 21 days for atrazine [36]. Another property of atrazine relevant to the modeling approach is that uptake by corn plants can be neglected [25]. According to the framework develop in Section 2, atrazine has therefore $\alpha = 0$ for this particular application.

All the other hydrological datasets used for the case study are summarized in Table .1. Precipitation measurements recorded in the Mönchaltorf area are provided by the cantonal office for environment AWEL (Zürich). Meteorological data for the Wädenswil station ($\sim$ 10 km from the study site) are taken from the database of the Federal Office of Meteorology and Climatology MeteoSwiss. Sunshine durations and air temperatures (used for computing potential evapotranspiration) and precipitation data are also provided by the same office.

3.2. Model

Model selection has been performed by progressively increasing the complexity of a lumped explicit soil moisture accounting [ESMA 11, 45] type of model until a satisfactory reproduction of the discharge and herbicides signal was achieved. The selected scheme is illustrated in Fig. .3. The overall water storage consists of an upper (S_u) and a lower (S_l) water specific storage (volume per unit area) whose temporal dynamics is described by the following differential equations:

$$\frac{dS_u}{dt} = nZ\frac{ds}{dt} = J(t) - J_e(t) - ET(t) \,, \tag{10}$$

$$\frac{dS_l}{dt} = R(t) - q_l(t) \,, \tag{11}$$

where $0 \leq s \leq 1$ is the soil moisture, n the soil porosity and Z the depth of the root zone (upper layer). Precipitation $J(t)$ represents the only input for the system and is assumed to infiltrate completely. Effective precipitation J_e is a nonlinear function of the soil moisture $J_e(t) = K_s \cdot s(t)^c$. A portion of the effective precipitation $R(t) = min(J_e(t), Re)$, where Re is the maximum recharge rate, drains into the lower storage. The remaining part is directly transformed into fast flow $q_u(t) = J_e(t) - R(t)$. The lower storage is modeled as a linear reservoir, i.e. $q_l(t) = k_l S_l(t)$, where k_l is a constant discharge rate. No surface runoff is explicitly accounted for; however, fast preferential flow due to macropores or drainage are conceptually modeled in the fast flow. Notice that more complex scheme (e.g. accounting for evapotraspiration form the lower storage) have been ruled out in the model selection as they performed similarly to the selected one but at a cost of a additional parameter.

Evapotranspiration $ET(t)$ is the sum of the output fluxes due to soil evapotranspiration and plant transpiration. In this study potential evapotranspiration ET_0 is estimated using the Priestley-Taylor [46] method, which

is a widely used radiation-based approach [e.g. 47] where only temperatures and the number of bright sunshine hours per day are needed. The actual evapotranspiration rate $ET(t)$, is assumed to be linearly increasing with the soil moisture s from $ET = 0$ at the wilting point s_w up to its maximum value $ET_0 K_c$, where K_c is a crop coefficient [48], at a suitable stress threshold s^*. Below s_w, ET is assumed to be null, while above s^* evapotranspiration proceeds unrestricted at its maximum value ($ET = ET_0 K_c$).

For the solute input a simple source model is considered [8, 30] where the application zone of atrazine is modeled as a near-surface domain responsible for most of the herbicide dynamics. Atrazine is applied to the soil surface and the mass applied $M_0(t)$ will be retained in a thin near-surface layer. To model the dynamics of mass depletion of atrazine within the source zone three processes are considered: i) sorption/desorption, ii) decomposition and iii) flushing by infiltrating rainfall. It is assumed that the sorption process is linear and reversible and that the equilibrium is reached instantaneously. Sorbed $N(t)$ and dissolved $C(t)$ concentration are linearly related by the distribution ratio K_d:

$$K_d = \frac{N(t)}{C(t)} = \frac{M_N(t)/M_{dry}}{M_C(t)/V_{water}}\,, \tag{12}$$

where $M_N(t)$ is the sorbed immobile mass, $M_C(t)$ is the dissolved mobile mass that can be leached by infiltrating rainfall, M_{dry} is the dry soil mass and V_{water} is the water volume within the soil. Manipulating Eq. (12) we can express $M_C(t)$ as a function of the total atrazine mass in the source zone ($M(t) = M_C(t) + M_N(t)$) as follow:

$$M_C(t) = \frac{M(t)}{1 + \frac{\rho K_d}{\theta}}\,, \tag{13}$$

where ρ is the bulk density and θ the volumetric water content.

Mass balance driving the temporal evolution of solute storage in the source zone gives:

$$\frac{dM(t)}{dt} \;=\; M_0(t) \;-\; kM(t) \;-\; \frac{M_C(t)}{\theta A Z_s}\, J(t)\,, \tag{14}$$

where $M_0(t)$ is the mass applied, k is the dissipation rate of the herbicide and Z_s the thickness of the source layer. The last term on the r.h.s. of Eq. (14) represents the mass flushed out of the source zone by the infiltrating rain.

For simplicity the source zone is assumed to be shallow hence immediately saturated upon arrival of rainfall events (i.e. $\theta = n$).

The concentration of organic soil components that can favor atrazine absorption in the deeper layers is assumed to be negligible with respect to the concentration in the near-surface zone. Therefore, atrazine exiting the source domain undergoes only degradation without further adsorption processes. To limit the number of parameters, it is assumed that the degradation rate k within the deeper layers is the same of the source zone (such assumption could be readily relaxed if deemed necessary). Therefore the herbicide mass out-flowing from the upper (ϕ_{J_e}) and lower (phi_l) storages is controlled by the ensuing (underlying) travel time distribution that dictates the time available for degradation and enrichment due to selective transpiration. Travel time distribution depends, in turn, on mixing processes and storage fluctuation induced by the hydrologic forcings. All these processes are accounted for in the general solution for the single control volume (9) that can thus be applied in series, first to the upper storage and after to the lower storage, to compute the respective mass fluxes ϕ_{J_e} and phi_l. In particular ϕ_{J_e} is computed substituting in Eq. (9) the corresponding storage, input and output fluxes ($I(t) = J(t)$, $Q(t) = J_e(t)$ and $S(t) = S_u(t)$) which have been computed using the hydrologic model develop for this specific case study (Eqs. 10 and 11) and setting $\alpha(t) = 0$ as discussed in Section 3.1. The resulting equation reads:

$$\phi_{J_e}(t) = -\int_{-\infty}^{t} J(t_i) C_0(t_i) \frac{J_e(t)}{S_u(t)} e^{-\int_{t_i}^{t} \frac{J_e(x)}{S_u(x)} dx - k(t-t_i)} dt_i \,, \tag{15}$$

where $C_0(t_i) = M_C(t_i)/(\theta A Z_s)$ is the solute concentration of the input precipitation after flowing through the source zone (Eq. 14). The solute flux ϕ_{J_e} is partitioned into ϕ_R and ϕ_u according to the same proportion as the water fluxes R and q_u. The flux ϕ_R is then considered as the input term of the lower storage. To apply the general solution (9) to this layer one thus has $I(t_i)C_I(t_i) = \phi_R(t_i)$, $Q(t) = q_l(t)$, $S(t) = S_l(t)$ and $\alpha(t) = 0$. The solute flux ϕ_l associated to the slow discharge q_l is thus computed as:

$$\phi_l(t) = -k_l \int_{-\infty}^{t} \phi_R(t_i) e^{-(k+k_l)(t-t_i)} dt_i \,, \tag{16}$$

where we have used the relation $q_l(x)/S_l(x) = k_l$ to simplify the equation.

3.3. Model Calibration

A total of 9 parameters (see Table .2) needs to be calibrated by contrasting the model outputs against observed data of both discharge and flux concentration. Calibration and sensitivity analysis has been performed using the Generalized Likelihood Uncertainty Estimation (GLUE) method [11]. To this end we have run 10^7 simulations with parameters randomly extracted from a uniform prior probability distribution spanning credible parameter ranges (see Table .2). For each model run, the Nash-Sutcliffe model efficiency is evaluated for both discharge (NS_Q) and concentration (NS_C) time series:

$$NS_Q = 1 - \frac{\sum_{t=1}^{T} \left(Q_o^t - Q_m^t\right)^2}{var(Q_o^t)} \tag{17}$$

$$NS_C = 1 - \frac{\sum_{p=1}^{P} \left(C_o^p - C_m^p\right)^2}{var(C_o^t)} \, . \tag{18}$$

In Eq. (17), Q_o^t and Q_m^t represent the observed and modeled mean daily discharge at day t, respectively; $T = 275$ is the total number of sampled days. Q_m^t is evaluated first by multiplying the total specific discharge by the catchment area ($Q_m(t) = (q_u(t) + q_l(t))A$) and then by computing the daily mean. Analogously, in Eq. (18) C_o^p and C_m^p are the modeled and observed average atrazine concentration in the equal flow-volume period p (see description in section 3.1); $P = 48$ is the total number of periods. Simulated flux concentration is computed as $C_m(t) = (\phi_u(t) + \phi_l(t))/(q_u(t) + q_l(t))$. A flow-weighted average is then performed over the equal flow-volume periods to obtain the C_m^p values.

As proposed by Beven [11], we use the Hornberger-Spear-Young method to calibrate and estimate the sensitivity of parameters: the Monte Carlo simulations are classified into behavioral and non-behavioral subsets on the basis of their goodness of fit. In particular each simulation, and hence the associated parameter set, is classified as behavioral when the efficiency NS_Q and NS_C are simultaneously greater than 0.82 and 0.52, respectively. These thresholds correspond to the 95 percentile of the Nash-Sutcliffe index distributions and lead to a count of 1451 behavioral sets. Finally, the procedure does not select a single simulation as the best one, whereas the ensemble of all the behavioral parameter sets is considered as a possible model parametrization. Model sensitivity to each parameter can be evaluated looking at its probability of occurrence in the behavioral subset. The larger the difference

with respect to an uniform distribution, the higher the sensitivity of the model results to that parameter.

The time constant of the lower storage $1/k_l$ was initially included in the calibration process. However a clear parameter range could not be identified because behavioral simulations for any value of $1/k_l$ larger than 90 days (without any upper bound) could be achieved. This is explained by noticing that for such low values of discharge rates, the lower storage is at stationary conditions endowed with nearly constant outflow equal to the mean recharge input. Moreover, when the travel time exceeds, say, three times the atrazine half-life (DT_{50}), most of the solute input ϕ_R is degraded inside S_l and the solute output ϕ_l is almost null. Therefore model results in terms of water and atrazine fluxes remain approximatively the same for any value of $1/k_l$ larger than 90 days and it is thus clear why an upper bound for this parameter cannot be identified. To reduce the dimensionality of the problem we then fixed $1/k_l = 90$ days and we focused the calibration on the remaining 9 parameters.

4. Results and Discussion

Fig. .4 shows the frequency distributions of the behavioral parameter sets. The corresponding model outputs are compared with the measured data in Fig. .5, where model results are represented by the median of all the behavioral simulations. While the agreement of the hydrological signal (panel b) is good, herbicide flux concentrations are instead reproduced less accurately. Given the complexity of the processes controlling concentration fluctuations, however, our results are deemed satisfactory. In particular the model proves reliable in reproducing two characteristic timescales of measured herbicide concentrations: a long timescale related to the persistence of solute components in soil and a shorter one related to the fluctuations induced by storm inter-arrivals. From Fig. .4 it can be noticed that model results are particularly sensitive to the maximum water storage in the upper layer (nZ) and the atrazine half-life (DT_{50}). The former, in fact, controls the time spent in the system while the latter controls herbicide degradation. Together, therefore, they control the total export of atrazine in the runoff. Our results are not very sensitive to the parameters that control evapotranspiration (s^* and K_c). This is likely due to the fact that different pairs of the two parameters can lead to reasonable estimates of the actual evapotranspiration. In future applications these parameters could thus be excluded form

the calibration procedure and reliably assumed based on literature values for the type of soil considered.

Fig. .4 also shows the frequency distributions of the hydrological parameters resulting from the calibration of the discharge signal alone (solid black line). These distributions have been obtained by selecting all the parameter sets matching the goodness of fit criteria for the discharge ($NS_Q > 0.82$), regardless of their performances in simulating the atrazine export. It can be noticed that the uncertainty of the hydrological parameters is significantly reduced when discharge and concentration are fitted simultaneously. Chemical data contain in fact information that allow for a better understanding of flow paths and hydrological processes and thus to significantly reduce the equifinality of model results.

It is interesting to analyze in detail the role of the parameter Re that quantifies the maximum recharge rate from the upper to the lower storage. It is not sensitive as far as the reproduction of the discharge is concerned (i.e. black line distribution in Fig. .4 is close to a uniform one) but it becomes important when one wants to capture correctly also the atrazine transport features (i.e. filled bars distribution is significantly different from a uniform one). The recharge flux ($R(t) = min(Re, J_e(t))$) is subtracted from the fast flow ($q_u(t) = J_e(t) - R(t)$) and released back to the river as slow flow from the lower storage ($q_l(t)$). In the behavioral simulations $J_e(t)$ is usually larger than Re so that the recharge $R(t)$ is constant and equal to the maximum rate Re and thus the lower storage reaches a stationary state with the output equal to the input: $q_l(t) = R(t) = Re$. As a result the total specific discharge ($q_l(t) + q_u(t)$) is independent of the value of Re and this explains the lack of sensitivity of the results to this parameter. The partition into two different storages is therefore not necessary to model discharge time series in this catchment but is crucial to reliably model the export of herbicides because the two flow components portray completely different chemical compositions. In fact, while the fast flow ($q_u(t)$) can carry a significant amount of atrazine, the water composing the slow flow ($q_l(t)$) has been retained in the system long enough for the solute to be almost completely degraded. The peaks and the droops of atrazine flux concentration in the streamflow (Fig. .5c) are controlled by the relative proportion of fast and slow flows: during rainfall events fast flow dominates and thus the total concentration increases, whereas during dry periods the discharge is largely contributed by slow flow and the concentration consequently decreases. Finally, the parameter distributions in Fig. .4 show how the flow from the lower storage (approximately equal to Re)

is much less than the K_s, the maximum flow from the upper storage. This result suggests that the two layers should be thought of as far apart one from the other with the upper storage modeling root zone dynamics on the lower storage mimicking a deep reservoir that contributes to stream base-flow.

The calibrated model offers the opportunity to investigate in detail the processes that control the export of atrazine and to disentangle the different roles of the underlying transport mechanisms. To this aim we track the fate of a pulse of solute in the upper layer by performing an instantaneous injection of a mass of solute (i.e. $\phi_J(t) = M_0\delta(t - t_0)$, where M_0 is the mass of solute, $\delta(\cdot)$ the Dirac delta distribution and t_0 the injection time) and by observing the corresponding normalized breakthrough curve $\phi_{J_e}(t)/M_0$. To assess the role played by the different mechanisms (e.g. solute degradation, travel time in the system, enrichment by evapotranspiration) we have repeated this virtual experiment with three solutes characterized by different chemical and physical properties: i) atrazine with the calibrated chemical parameters; ii) a conservative solute that is not taken up by evapotranspiration ($k = 0$, $\alpha = 0$) and iii) a conservative solute that is taken up by evapotranspiration ($k = 0$, $\alpha = 1$). The second type of solute may behave similarly to chloride which is weakly uptaken by plants. The third type of solute has the same properties of the water carrier and is thus useful to measure the delay of the breakthrough curve that is exclusively due to convection and mixing, as quantified by the water travel time in the system. All the other fluxes and parameters are the observed and calibrated ones, respectively. The three different breakthrough curves are reported in Fig. .6. Only 60% of the atrazine (green line) is collected in the outflow because the remaining fraction has been degraded inside the system. In the case of the water (blue line) 80% of the injected mass exits as J_e while the remaining part is evapotranspired. This breakthrough curve is by definition proportional to the water travel time in the upper storage. Mathematically this can be derived by recalling Eq. (9) particularized to the case at hand (i.e. $I \equiv J$, $J_e \equiv Q$, $I(t_i)C_I(t_i) = M_0\delta(t_i - t_0)$, $\alpha = 1$ and $k = 0$) and Eq. (8). Indeed one gets $\phi_{J_e}(t)/M_0 = \theta(t_0)p_t(t - t_0|t_0)$, where $\theta(t_0)$, i.e. the fraction of particles leaving the system as J_e, is equal to the 80% as illustrated above. Finally, in the case of the solute not taken up by transpiration (red curve), the breakthrough curve carries 100% of the mass injected. Such curve can be thought of as the travel time pdf of solutes particles. It is important, however, to highlight the difference between the travel time pdfs of water (blue line) and of the third type of solute (red line). The difference is fundamentally due to the fact that while the water

can follow two pathways to the exit (flow and evapotranspiration), the considered solute just one (flow). As a consequence, solutes with low affinity to evapotranspiration are usually retained longer in the system.

This simple example carries relevant hydrological implications. Isotopes, chloride and other tracers have been in fact widely used in the literature [e.g. 17, 19, 49] to infer water travel time distributions. However, theoretical arguments and numerical simulations clearly show that different tracer affinity to be taken up by plants can significantly bias the interpretation of the results in terms of water travel times. The role of evapotranspiration cannot be overlooked a priori. Its effect can be limited, although hardly negligible, in wet climates where streamflows represent the biggest component of the water budget, but it becomes dominant in semi-arid to arid climates.

We now examine the effects of stochasticity of rainfall patterns and herbicides application dates on water quality dynamics and the related ecotoxicological risk. A general consensus exists, for instance, on the fact that the first intense rain events after application determine most of herbicide losses to surface waters [e.g. 27]. To investigate this effect and to assess the probability distribution of atrazine loads and other variables crucial for river ecosystems, we set up a series of Monte Carlo simulations combining the calibrated model with a stochastic model for rainfall generation. We use a simple stochastic model of daily precipitation [50], which describes the occurrence of rainfall events as a compound Poisson process and rainfall depths as an exponentially distributed random variable. The model is calibrated on a monthly basis using a 20-years long time series of daily precipitation available at a nearby station (see Table .1). For every year of simulation, atrazine application is assumed to occur during a single day which is randomly selected among all the non-rainy days in the period permitted by Swiss law (May 1^{st}–June 30^{th}). We run a 10^4-years long Monte Carlo simulation (Fig. .7a shows a 3-year sample of atrazine concentration). The corresponding probability distributions of the percentage of applied atrazine mass that is annually exported to surface water are presented in Fig. .7b. The red line distribution is obtained analyzing all the years of the simulation. Green and blue lines are instead derived selecting only the years where the period between the herbicide application and the first intense rainfall events (> 5 mm/day) is longer than 2 and 5 days, respectively. Results reveal that the delay of the first rainfall events after the herbicides application has indeed an effect on the total export: the longer the delay, the smaller the yearly load. Thus farmers, supported by reliable weather forecasts, can improve their managing practices

in order to avoid rainfall events after crop treatments with atrazine. This practice has two major benefits: i) increasing herbicide efficiency as crop protection because it remains longer in the soil and ii) reducing herbicides export to surface water.

Traditional approach to ecological risk assessment of aquatic communities has focused on the chronic exposure to constant concentration of herbicides. However, as highlighted also in this study, concentrations in natural aquatic environments are typically irregular, punctuated by pulses characterized by pronounced peaks (well above the long-term water quality standards defined to protect the aquatic organisms). For these reasons, recent studies [32–34] started to investigate the ecological risk related to varying herbicide concentration testing, in particular, the effects of subsequent peaks of concentration followed by recovery periods. These studies propose that the key variables that can quantify the ecotoxicological risk induced by the exposure of herbicides are the frequency and the duration of peaks of concentration over a certain critical threshold and the duration of the subsequent recovery periods. The Monte Carlo framework developed herein directly allows a probabilistic analysis of this key variables (see example in Fig. .7a) providing a valuable tool for ecological risk assessment.

5. Conclusions

A recently developed theoretical framework for deriving time-variant travel time distributions has been extended to characterize herbicides transport at catchment scales. The effect of mixing processes of water of different ages is investigated, in particular by assuming that mobilization of soil water involves randomly sampled particles from the available storage.

An analytical expression for the evolution of the concentration has been derived by taking into account partial uptake of solutes by evapotranspiration and first-order degradation reactions. The model developed allows to express analytically solute fluxes leaving a catchment in terms of the underlying soil moisture dynamics and the input concentrations. Differences of residence times for water compared to those of solutes are addressed.

The transport model for atrazine is applied to the Aabach-Mönchaltorf catchment (Switzerland). The calibrated model provides satisfactory results in estimating temporal trends compared to the measured signals, suggesting the robustness of the well mixed assumption in modeling catchment scale circulation of solutes.

Tools for ecological risk assessment, such the evaluation of total load or duration and extent of crossings of pre-defined concentrations, are computed via a probabilistic analysis using Monte Carlo simulations.

Appendix A.

This appendix details the analytical derivation of the travel time distribution under the well-mixed assumption. By definition, $I(t_i)dt_iP(t-t_i|t_i)$ is the infinitesimal volume of water entered in the time interval $[t_i, t_i+dt_i]$ that is still contained in the control volume V at time t. If water particles of both Q and ET fluxes are randomly sampled among all the water particles in V, the time evolution of such infinitesimal volume can be written as:

$$\frac{d(I(t_i)dt_iP(t-t_i|t_i))}{dt} = -(Q(t)+ET(t))\frac{I(t_i)dt_iP(t-t_i|t_i)}{S(t)}. \tag{A.1}$$

Eq. (A.1) expresses that the probability for the out-fluxes Q and ET to sample particles entered in the time interval $[t_i, t_i+dt_i]$ is equal to the relative fraction of such particles with respect to the total storage $I(t_i)dt_iP(t-t_i|t_i)/S(t)$. Solving Eq. (A.1) with the initial condition $P(0|t_i)=1$ we obtain an analytical solution for $P(t-t_i|t_i)$ as a function of the water storage S and of the hydrologic forcings Q and ET:

$$P(t-t_i|t_i) = e^{-\int_{t_i}^{t}\frac{Q(x)+ET(x)}{S(x)}dx}. \tag{A.2}$$

The travel time pdf $p_t(t-t_i|t_i)$ $t>t_i$ can be derived, by definition, as the normalized outflux as Q of particles that have entered the system in the time interval $[t_i, t_i+dt_i]$. Recalling Eqs. (A.1) and (A.2), this translates into

$$p_t(t-t_i|t_i) = \frac{Q(t)}{S(t)\theta(t_i)}e^{-\int_{t_i}^{t}\frac{Q(x)+ET(x)}{S(x)}dx}\ , \tag{A.3}$$

where $\theta(t_i)$ is the normalization factor:

$$\theta(t_i) = \int_{t_i}^{\infty}\frac{Q(t)}{S(t)}e^{-\int_{t_i}^{t}\frac{Q(x)+ET(x)}{S(x)}dx}dt\ , \tag{A.4}$$

which, as introduced above, represents the fraction of water particles entered in the time interval $[t_i, t_i+dt_i]$ that will exit as Q. Notice that the value of $\theta(t_i)$ depends, as expected, on the whole sequence of hydrologic forcing occurring after t_i.

Appendix B.

Under the hypotheses stated in section 3, it is possible to define $I(t_i)dt_iP(t-t_i|t_i)C(t-t_i,t_i)$ as the infinitesimal solute mass entered in the time interval $[t_i, t_i+dt_i]$ that is contained in the control volume V at time t. Under the well-mixed assumption, the time evolution of such infinitesimal mass can be written as:

$$\begin{aligned} & \frac{d}{dt}(I(t_i)dt_iP(t-t_it_i)C(t-t_i,t_i)) = \\ - \quad & Q(t)\,\frac{I(t_i)dt_iP(t-t_i|t_i)}{S(t)}C(t-t_i,t_i) + \\ - \quad & ET(t)\frac{I(t_i)dt_iP(t-t_i|t_i))}{S(t)}\alpha(t)C(t-t_i,t_i) \; + \\ - \quad & kI(t_i)dt_iP(t-t_i|t_i)C(t-t_i,t_i)\,, \end{aligned} \tag{B.1}$$

where the first and the second terms on the right hand side express the solute out-fluxes due to discharge and evaporation, respectively. The last term in Eq. (B.1) quantifies the solute mass degraded. Using Eq. (A.1), Eq. (B.1) simplifies to the differential equation:

$$\frac{dC(t-t_i,t_i)}{dt} = \frac{ET(t)}{S(t)}(1-\alpha(t))C(t-t_i,t_i) - kC(t-t_i,t_i)\,; \tag{B.2}$$

the solution of which is:

$$C(t-t_i,t_i) = C_I(t_i)e^{\int_{t_i}^{t}\frac{(1-\alpha(t))ET(x)}{S(x)}dx - k(t-t_i)}\,, \tag{B.3}$$

where $C_I(t_i) = C(0,t_i)$ is the initial solute concentration in the input I. According to Eq. (B.3), the solute concentration of each water pulse is enriched by selective evapotraspiration and decreased by decay/degradation.

Inserting Eqs. (B.3) and (8) into Eq. (7) we obtain the relation

$$\phi_Q(t) = \int_{-\infty}^{t} I(t_i)C_I(t_i)\frac{Q(t)}{S(t)}e^{-\int_{t_i}^{t}\frac{Q(x)+\alpha(x)\,ET(x)}{S(x)}dx - k(t-t_i)}dt_i\,, \tag{B.4}$$

which concludes the derivation.

References

[1] M. Brusseau, P. Rao, Sorption Nonideality During Organic Contaminant Transport In Porous-Media, Critical Reviews In Environmental Control 19 (1) (1989) 33–99.

[2] M. Flury, Experimental evidence of transport of pesticides through field soils - A review, Journal of Environmental Quality 25 (1) (1996) 25–45.

[3] K. J. McGuire, J. J. McDonnell, A review and evaluation of catchment transit time modeling, Journal Of Hydrology 330 (3-4) (2006) 543–563.

[4] B. Bird, W. Stewart, Lightfoot, Transport Phenomena, Johns & Sons, New York, 1960.

[5] A. Rinaldo, A. Marani, Basin Scale-Model Of Solute Transport, Water Resources Research 23 (11) (1987) 2107–2118.

[6] A. Rinaldo, A. Marani, A. Bellin, On Mass Response Functions, Water Resources Research 25 (7) (1989) 1603–1617.

[7] N. Haws, P. Rao, J. Simunek, I. Poyer, Single-porosity and dual-porosity modeling of water flow and solute transport in subsurface-drained fields using effective field-scale parameters, Journal of Hydrology 313 (3-4) (2005) 257–273.

[8] S. Zanardo, N. B. Basu, G. Botter, A. Rinaldo, S. P. Rao, Dominant controls on pesticide transport from tile to catchment scale: Lessons from a minimalist model, *in press* Water Resources Research-doi:doi:10.1029/2010WR010088.

[9] J. McDonnell, A Rationale For Old Water Discharge Through Macropores In A Steep, Humid Catchment, Water Resources Research 26 (11) (1990) 2821–2832.

[10] A. Rodhe, L. Nyberg, K. Bishop, Transit times for water in a small till catchment from a step shift in the oxygen 18 content of the water input, Water Resources Research 32 (12) (1996) 3497–3511.

[11] K. J. Beven, Rainfall - Runoff Modelling: The Primer, John Wiley & Sons, New York, 2001.

[12] J. J. McDonnell, K. McGuire, P. Aggarwal, K. J. Beven, D. Biondi, G. Destouni, S. Dunn, A. James, J. Kirchner, P. Kraft, S. Lyon, P. Maloszewski, B. Newman, L. Pfister, A. Rinaldo, A. Rodhe, T. Sayama, J. Seibert, K. Solomon, C. Soulsby, M. Stewart, D. Tetzlaff, C. Tobin, P. Troch, M. Weiler, A. Western, A. Worman, S. Wrede, How old is streamwater? Open questions in catchment transit time conceptualization, modelling and analysis, Hydrological Processes 24 (12, Sp. Iss. SI) (2010) 1745–1754.

[13] G. Botter, E. Bertuzzo, A. Rinaldo, Transport in the hydrologic response: Travel time distributions, soil moisture dynamics, and the old water paradox, Water Resources Research 46 (2010) W03514.

[14] G. Dagan, Flow and Transport in Heterogeneous Porous Formations, Springer-Verlag, Berlin, 1987.

[15] M. Stewart, J. McDonnell, Modeling base-flow soil-water residence times from deuterium concentrations, Water Resources Research 27 (10) (1991) 2681–2693.

[16] D. Burns, J. McDonnell, R. Hooper, N. Peters, J. Freer, C. Kendall, K. Beven, Quantifying contributions to storm runoff through end-member mixing analysis and hydrologic measurements at the Panola Mountain Research Watershed (Georgia, USA), Hydrological Processes 15 (10) (2001) 1903–1924.

[17] M. Hrachowitz, C. Soulsby, D. Tetzlaff, J. J. C. Dawson, S. M. Dunn, I. A. Malcolm, Using long-term data sets to understand transit times in contrasting headwater catchments, Journal of Hydrology 367 (3-4) (2009) 237–248.

[18] M. Hrachowitz, C. Soulsby, D. Tetzlaff, J. J. C. Dawson, I. A. Malcolm, Regionalization of transit time estimates in montane catchments by integrating landscape controls, Water Resources Research 45 (2009) W05421.

[19] M. Hrachowitz, C. Soulsby, D. Tetzlaff, M. Speed, Catchment transit times and landscape controls-does scale matter?, Hydrological Processes 24 (1) (2010) 117–125.

[20] D. Tetzlaff, C. Soulsby, M. Hrachowitz, M. Speed, Relative influence of upland and lowland headwaters on the isotope hydrology and transit times of larger catchments, Journal of Hydrology 400 (3-4) (2011) 438–447.

[21] P. Rao, R. Green, Balasub.V, Y. Kanheiro, Field Study Of Solute Movement In A Highly Aggregated Oxisol With Intermittent Flooding 2. Picloram, Journal of Environmental Quality 3 (3) (1974) 197–202.

[22] W. Jury, H. Elabd, M. Resketo, Field-Study Of Napropamide Movement Through Unsaturated Soil, Water Resources Research 22 (5) (1986) 749–755.

[23] P. Squillace, E. Thurman, Herbicide transport in rivers - importance of hydrology and geochemistry in nonpoint-source contamination, Environmental Science & Technology 26 (3) (1992) 538–545.

[24] M. Flury, J. Leuenberger, B. Studer, H. Fluhler, Transport Of Anions And Herbicides In A Loamy And A Sandy Field Soil, Water Resources Research 31 (4) (1995) 823–835.

[25] H. Alvord, R. Kadlec, Atrazine fate and transport in the Des Plaines Wetlands, Ecological Modelling 90 (1) (1996) 97–107.

[26] K. Hyer, G. Hornberger, J. Herman, Processes controlling the episodic steamwater transport of atrazine and other agrichemicals in an agricultural watershed, Journal Of Hydrology 254 (1-4) (2001) 47–66.

[27] C. Stamm, C. Waul, C. Leu, L. Freitas, G. Popow, H. Singer, S. Muller, Sorption effects on herbicide losses to surface waters in a small catchment of the Swiss Plateau, Zeitschrift Fur Pflanzenkrankheiten Und Pflanzenschutz-Journal Of Plant Diseases And Protection (2004) 951–958.

[28] W. Ling, J. Xu, Y. Gao, Dissolved organic matter enhances the sorption of atrazine by soil, Biology And Fertility Of Soils 42 (5) (2006) 418–425.

[29] M. Larose, G. C. Heathman, L. D. Norton, B. Engel, Hydrologic and atrazine simulation of the cedar creek watershed using the SWAT model, Journal of Environmental Quality 36 (2) (2007) 521–531.

[30] G. S. McGrath, C. Hinz, M. Sivapalan, Modeling the effect of rainfall intermittency on the variability of solute persistence at the soil surface, Water Resources Research 44 (9).

[31] R. Siber, C. Stamm, P. Reichert, Modeling potential herbicide loss to surface waters on the Swiss plateau, Journal Of Environmental Management 91 (1) (2009) 290–302.

[32] N. Vallotton, R. Ilda, L. Eggen, B. I. Escher, J. Krayenbuehl, N. Chevre, Effect of pulse herbicidal exposure on scenedesmus vacuolatus: A comparison of two photosystem ii inhibitors, Environmental Toxicology and Chemistry 27 (6) (2008) 1399–1407.

[33] N. Vallotton, R. I. L. Eggen, N. Chevre, Effect of sequential isoproturon pulse exposure on scenedesmus vacuolatus, Archives of Environmental Contamination and Toxicology 56 (3) (2009) 442–449.

[34] A. Tlili, B. Montuelle, A. Berard, A. Bouchez, Impact of chronic and acute pesticide exposures on periphyton communities, Science of the Total Environment 409 (11) (2011) 2102–2113.

[35] C. Leu, H. Singer, C. Stamm, S. Muller, R. Schwarzenbach, Simultaneous assessment of sources, processes, and factors influencing herbicide losses to surface waters in a small agricultural catchment, Environmental Science & Technology 38 (14) (2004a) 3827–3834.

[36] L. G. Freitas, H. Singer, S. R. Mueller, R. P. Schwarzenbach, C. Stamm, Source area effects on herbicide losses to surface waters - A case study in the Swiss Plateau, Agriculture Ecosystems & Environment 128 (3) (2008) 177–184.

[37] M. P. Frey, M. K. Schneider, A. Dietzel, P. Reichert, C. Stamm, Predicting critical source areas for diffuse herbicide losses to surface waters: Role of connectivity and boundary conditions, Journal Of Hydrology 365 (1-2) (2009) 23–36.

[38] C. Leu, H. Singer, C. Stamm, S. Muller, R. Schwarzenbach, Variability of herbicide losses from 13 fields to surface water within a small catchment after a controlled herbicide application, Environmental Science & Technology 38 (14) (2004) 3835–3841.

[39] P. Capel, S. Larson, T. Winterstein, The behaviour of 39 pesticides in surface waters as a function of scale, Hydrological Processes 15 (7) (2001) 1251–1269.

[40] N. Chevre, C. Loeppe, H. Singer, C. Stamm, K. Fenner, B. Escher, Including mixtures in the determination of water quality criteria for herbicides in surface water, Environmental Science & Technology 40 (2) (2006) 426–435.

[41] C. Leu, H. Singer, S. Muller, R. Schwarzenbach, C. Stamm, Comparison of atrazine losses in three small headwater catchments, Journal Of Environmental Quality 34 (5) (2005) 1873–1882.

[42] G. Botter, E. Bertuzzo, A. Rinaldo, Catchment residence and travel time distributions: The master equation, Geophysical Research Letters 38 (2011) L11403.

[43] A. Rinaldo, K. Beven, E. Bertuzzo, L. Nicotina, J. Davies, A. Fiori, D. Russo, G. Botter, Catchment travel time distributions and water flow in soils, Water Resources Research 47 (2011) W07537.

[44] N. Chévre, Evaluation du risque des pesticides : Dans les eaux courantes en Suisse, GWA. Gas, Wasser, Abwasser 84 (10) (2004) 739–751.

[45] P. O'Connell, A historical perspective, in: D. Bowles, P. O'Connell (Eds.), Recent Advances in the Modeling of Hydrologic Systems, Kluwer Academic Publishers, The Netherlands, 1991, pp. 3–30.

[46] C. Priestley, R. Taylor, Assessment of Surface Heat-Flux and Evaporation Using Large-Scale Parameters, Monthly Weather Review 100 (2) (1972) 81–92.

[47] C. Xu, D. Chen, Comparison of seven models for estimation of evapotranspiration and groundwater recharge using lysimeter measurement data in Germany, Hydrological Processes 19 (18) (2005) 3717–3734.

[48] R.-G. Allen, L.-S. Pereira, D. Raes, M. Smith, Crop evapotranspiration. guidelines for computing crop water requirements, FAO Irrigation and Drainage Papers 56.

[49] J. Kirchner, X. Feng, C. Neal, Fractal stream chemistry and its implications for contaminant transport in catchments, Nature 403 (6769) (2000) 524–527.

[50] I. Rodriguez-Iturbe, A. Porporato, L. Ridolfi, V. Isham, D. Cox, Probabilistic modelling of water balance at a point: the role of climate, soil and vegetation, Proceedings of the Royal Society A-Mathematical Physical and Engineering Sciences 455 (1990) (1999) 3789–3805.

Table .1: Available Data for the Mönchaltorf Catchment. WAE stands for Wdenswil and MOE for Mönchsaltorf. The W denswil station is situated approximately 10 kilometers from the study site.

Station	Parameter	Time Step	Period
MOE	Discharge; daily mean	day	1999
MOE	Precipitation; daily total	day	1999
MOE	Atrazine Concentration	day	1999
WAE	Sunshine duration; daily total	day	1999
WAE	Air temperature; daily mean	day	1999
WAE	Precipitation; daily total	day	1990-2009

Table .2: Calibration Parameters and interval explored in the GLUE analysis

Parameter	Variable name	Lower bound	Upper bound
pore volume in the root zone	nZ $[m]$	0.04	0.5
stress threshold for ET	s^*	0.3	0.5
non-linear reservoir parameter	K_s $[mmh^{-1}]$	25	500
non-linear reservoir exponent	c	3	8
crop coefficient	K_c	0.5	2
recharge rate	Re $[mmd^{-1}]$	0.2	2
atrazine half-life	DT_{50} $[d]$	10	30
depth of the source layer	Z_s $[m]$	0.02	0.2
distribution ratio	K_d $[lkg^{-1}]$	2	10

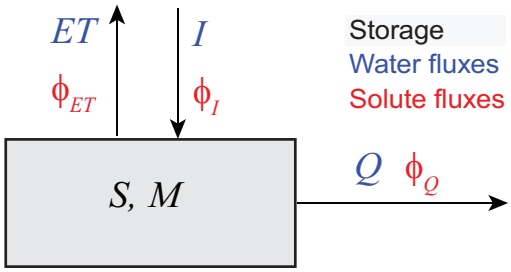

Figure .1: Conceptual scheme of the hydrologic unit considered in the theoretical framework.

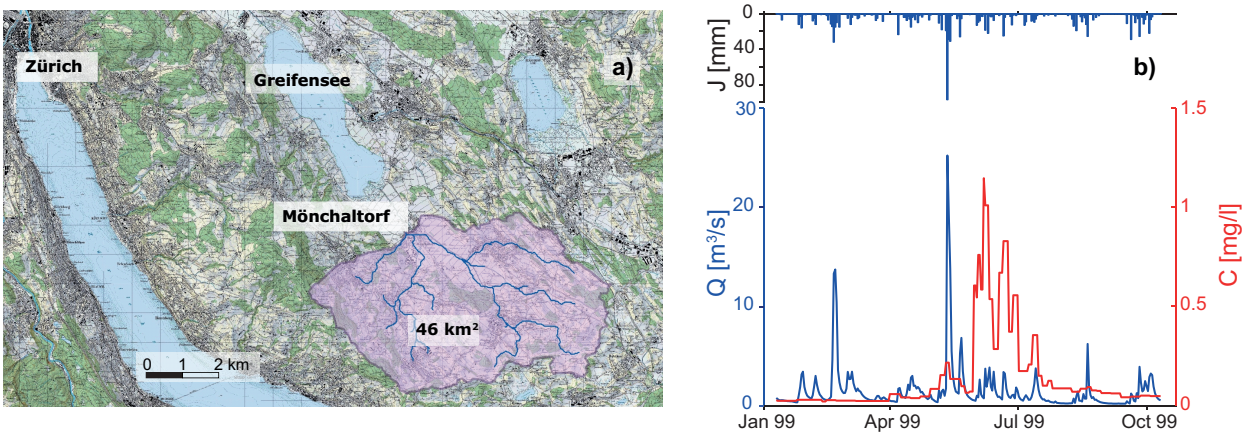

Figure .2: a) Map of the study area. The Aabach-Mönchsaltorf catchment is shown in color. b) Dynamics of discharge Q and atrazine concentration C measured in the brook Aabach in Mönchaltorf [data from 40, 44].

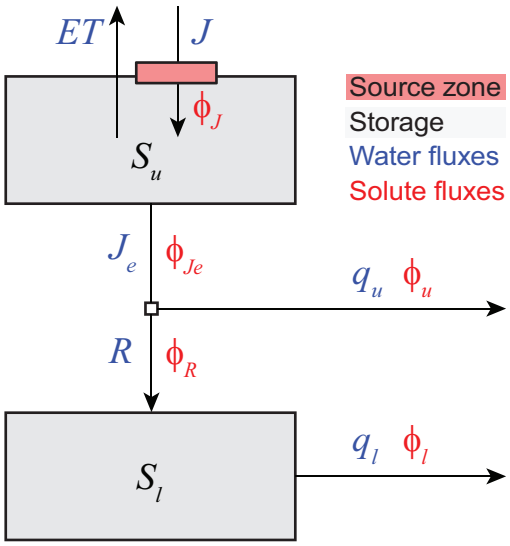

Figure .3: Conceptual scheme of the model used for the atrazine transport in the Aabach-Mönchaltorf catchment. The upper storage receives as input the overall rainfall J and solutes that are flushed out of the source zone layer ϕ_J. This produces as output the evapotranspiration water flux ET, the water flux J_e and the associated solute flux ϕ_{J_e}. Part of J_e is directly transformed into the fast flow component of the streamflow q_u, with the associated solute flux ϕ_u. Part of J_e contributes to the recharge R of the lower storage that returns as the slow flow component of the streamflow q_l.

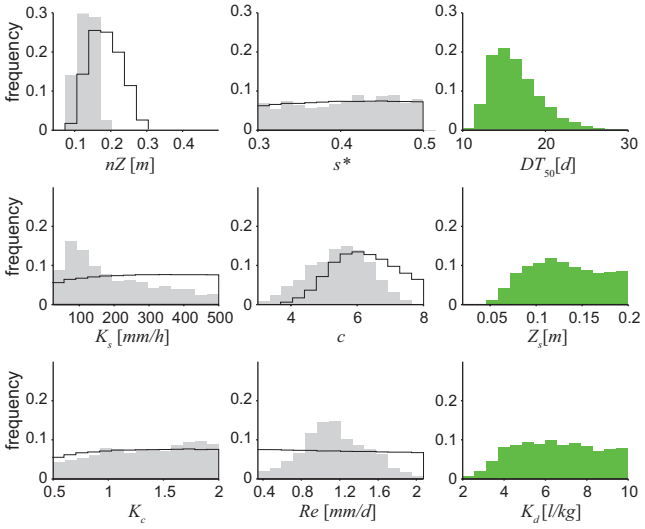

Figure .4: Parameter distributions. Filled bars show the distributions for the behavioral set of simulations with $NS_Q > 0.82$ and $NS_C > 0.52$. Green bars highlight the three parameters of the herbicides transport model. Black lines show the parameter distributions of all the simulations with $NS_Q > 0.82$, i.e. when only the discharge time series is used to calibrate the hydrological model. The comparison shows that calibrating simultaneously discharge and concentration decreases the uncertainty in the estimation of the hydrological parameters.

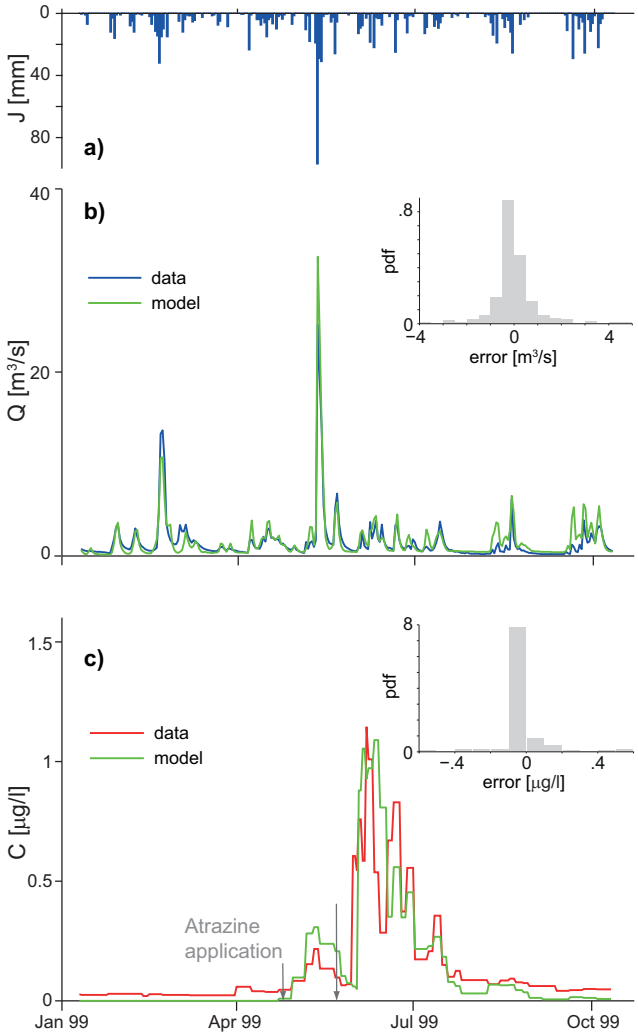

Figure .5: Comparison between simulated and measured hydrographs and chemographs: (a) Rainfall data, (b) Discharge data (blue) versus model (green), (c) Concentration data (red) versus model (green). The arrows indicate the dates of modeled atrazine application. Insets in (a) and (b) show the probability distribution of the differences between model and data.

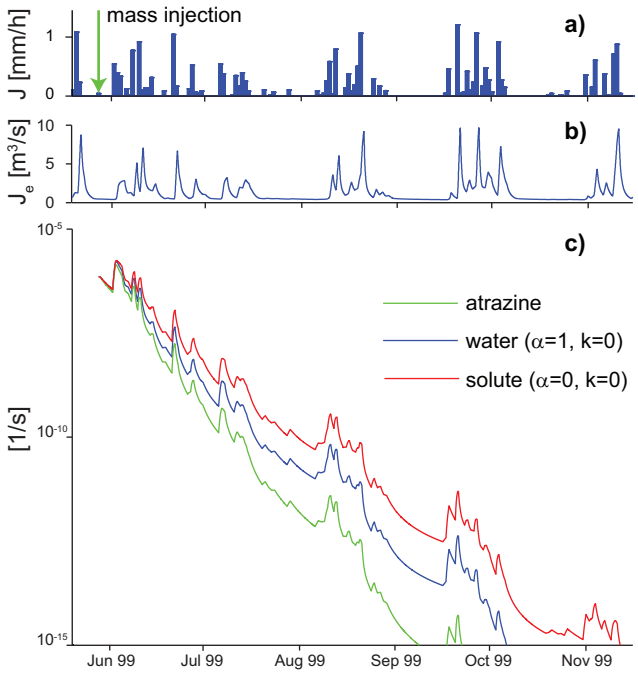

Figure .6: Breakthrough curves due to an instantaneous injection of a mass of solutes in the upper layer of the model (c). (a) and (b) show the time series of the forcing precipitation and the flow release by the upper layer, respectively. The time of the injection is also shown in (a). Three different solute are considered: atrazine (green line), a conservative solute that is not uptaken by evapotranspiration ($k = 0$, $\alpha = 0$; red line) and a conservative solute that is uptaken by evapotranspiration ($k = 0$, $\alpha = 1$; blue line). The latter solute has the same properties of the carrier water.

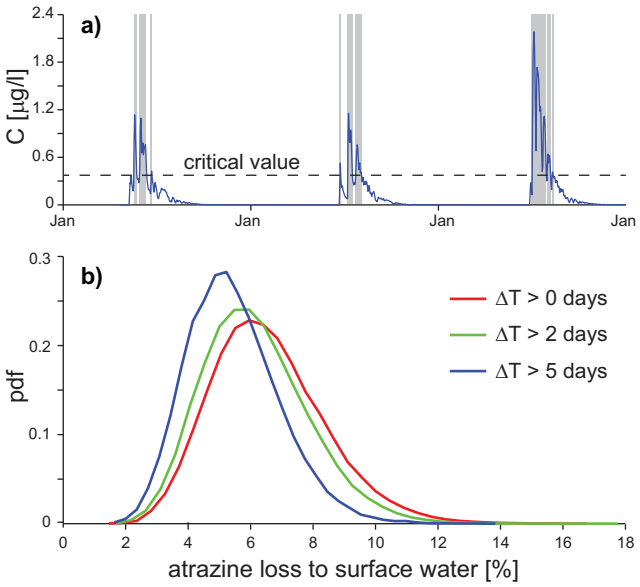

Figure .7: Monte Carlo simulation of atrazine dynamics with stochastic precipitation patterns and application dates. a) Example of a 3-year long simulation of atrazine concentration time series with illustration of the method to calculate the statistics of the timespans over a critical threshold. b) Probability distributions of the percentage of applied atrazine mass that is annually exported to surface water obtained form a 10^4-years long simulation. Green and blue lines refer to the distributions derived selecting only the years where the period between the herbicide application and the first intense rainfall events (> 5 mm/day) is longer than 2 and 5 days, respectively. Red line distribution is instead obtained analyzing all the years regardless of the time of occurrence of the first rainfall event.